

Quantitative spectral analysis of early B-type supergiants in the Sculptor galaxy NGC 300¹

Miguel Alejandro Urbaneja, Artemio Herrero², Fabio Bresolin, Rolf-Peter Kudritzki³,
Wolfgang Gieren⁴ and Joachim Puls⁵

ABSTRACT

The spectra of two early B-type supergiant stars in the Sculptor spiral galaxy NGC 300 are analysed by means of non-LTE line blanketed unified model atmospheres, aimed at determining their chemical composition and the fundamental stellar and wind parameters. For the first time a detailed chemical abundance pattern (He, C, N, O, Mg and Si) is obtained for a B-type supergiant beyond the Local Group. The derived stellar properties are consistent with those of other Local Group B-type supergiants of similar types and metallicities. One of the stars shows a near solar metallicity while the other one resembles more a SMC B supergiant. The effects of the lower metallicity can be detected in the derived wind momentum.

Subject headings: galaxies: individual (NGC 300) — stars: abundances, early-type, supergiants, fundamental parameters, winds, outflows

1. Introduction

The 8-10 meter class telescopes and their new generation instruments make it possible to extend the quantitative stellar spectroscopy beyond the Local Group. Early B-type su-

¹Based on observations obtained at the ESO Very Large Telescope

²Instituto de Astrofísica de Canarias, Vía Láctea S/N, E-38200 La Laguna, Canary Islands, Spain, maup@ll.iac.es, ahd@ll.iac.es; Dpto. de Astrofísica, Universidad de La Laguna, Avda. Astrofísico Francisco Sánchez, E-38271 La Laguna, Canary Islands, Spain, ahd@ll.iac.es

³Institute for Astronomy, University of Hawaii, 2680 Woodlawn Drive, Honolulu, Hawaii 96822, bresolin@ifa.hawaii.edu, kud@ifa.hawaii.edu

⁴Universidad de Concepción, Departamento de Física, Casilla 160-C, Concepción, Chile, wgieren@coma.cfm.udec.cl

⁵Universitäts-Sternwarte München, Scheinerstr. 1, D-81679 München, Germany, uh101aw@usm.uni-muenchen.de

pergiant stars are ideal targets for detailed spectroscopy even at low resolution ($R \sim 1000$). Their blue spectra are rich in metal features which allows us the analysis of chemical species like C, N, O, Si and Mg. Although our knowledge of the evolution of massive stars still has open questions, most of the recent works indicate that the blue luminous supergiants do not show any contamination of their oxygen surface abundances during the early stages of their evolution, neither the O-types (Villamariz et al. 2002), nor the B-types (Smartt, Dufton, & Lennon 1997; Monteverde, Herrero, & Lennon 2000; Smartt et al. 2002), nor the A-types (Venn 1995; Takeda & Takada-Hidei 1998; Przybilla 2002), which enables a direct comparison between the stellar oxygen abundances and the ones derived from H II regions. This has become extremely important, especially in the extragalactic field where oxygen is used as the primary metallicity indicator, due to the fact that at high metallicity (larger than approx. 0.5 solar) strong line methods must be used, for which the choice of the calibration strongly influences the derived abundances (Kewley & Dopita 2002; Pilyugin 2002). In addition to chemical abundance studies, blue luminous stars have strong radiatively driven mass outflows which can provide us with information on extragalactic distances by means of the Wind Momentum - Luminosity Relationship, WLR (Kudritzki & Puls 2000, and references therein).

Recently, and within a wide program aimed at the spectroscopy study of luminous blue stars beyond the Local Group, first steps have been done for A-type supergiants in NGC 3621 (6.7 Mpc away, Bresolin et al. 2001). Quantitative spectroscopy has been shown to be possible for A-type supergiants (Bresolin et al. 2002a) and Wolf-Rayet stars (Bresolin et al. 2002b) in NGC 300, 2.02 Mpc away in the Sculptor group. Here we report the first quantitative analysis of B-type supergiants (hereafter B-Sg) out of the Local Group, presenting the detailed chemical pattern along with the stellar parameters and the wind properties. The technique will be applied in a forthcoming paper to a large set of early B-Sg located at several galactocentric distances in order to derive radial abundance gradients of the α -elements. Combined with the results of a similar study of A-type supergiants it will provide a wealth of information on the chemical evolution of the host galaxy NGC 300.

2. Observations

The stars are part of a spectroscopic survey of photometrically selected blue luminous supergiants in the Sculptor galaxy NGC 300, obtained at the VLT with the FORS multi-object spectrograph, and described in detail by Bresolin et al. (2002a), which presents a spectral catalog of 70 luminous blue supergiants in the blue region ($\sim 4000 - 5000 \text{ \AA}$). The selected stars are identified as B-12 and A-9 in that spectral catalog (see their Table 2 and

finding charts). In September 2001 the spectra of the $H\alpha$ region were obtained in order to measure the mass-loss rates, which provide us with a complete coverage of the 3800 - 7200 Å wavelength range at $R \sim 1000$ resolution. The reader is referred to Bresolin et al. (2002a) for a detailed description of the observations and reduction process, as well as for the photometry and the spectral classification of the stars.

3. Spectral analysis

The spectra of early B-Sg are dominated by the O II lines, followed by N II/N III, Si III/Si IV, C II/C III and Mg II, in addition to H and He I lines. At high resolution it is possible to detect some other metal lines of Al III, S II/S III and Fe III but, due to their intrinsic weakness, these lines do not have any influence in the analysis at low resolution and could hardly be used to fix the abundance of such elements. Fig. 1 shows the high resolution - high S/N ratio ($R \sim 15000$, $SNR \sim 350$) blue spectrum of the Galactic supergiant HD14956 (B1.5Ia), and the same spectrum degraded to the resolution of the NGC 300 data, $R \sim 1000$ (labeled as $\#d$ in the figure). We have also included the identification of the more important lines. As can be seen, only a few strong lines remain isolated at that low resolution, therefore the analysis must be based on the comparison of the observed spectra to a set of model atmospheres that include a vast number of lines in the calculation of the emergent fluxes. We have taken into account more than two hundreds metal lines in the 3800 - 6000 Å wavelength range. It is important to include extense metal line lists because of the fact that some spectral features are formed by the contribution of several chemical species (e.g. the strong blend of O, N and C at ~ 4650 Å). We have excluded some strong isolated lines because our atomic models do not consider the levels involved in these transitions. Nevertheless, these lines are isolated and have no influence on the results.

Even considering the noise effects in the lower resolution FORS spectra (displayed also in Fig. 1), strong metal features can still be detected and used for a detailed chemical abundance analysis. In particular a wealth of information can be extracted from the selected regions at 4070, 4320, 4420 (O II), 4550 - 4570 (Si III), 4600 - 4660 (O II, N II, N III and C III) and 5010 (N II and He I).

3.1. Atmosphere models

We use the newest version of the FASTWIND code (first presented by Santolaya-Rey, Puls, & Herrero 1997) which solves the radiation transfer in a moving media by means of

suitable approximations which simplify the numerical treatment of the problem but without affecting the physical significance of the results. The atmospheric structure is treated in a consistent way, assuming a β -velocity law in the wind, ensuring a smooth transition between the "photosphere" and the "wind"; the temperature structure is approximated by means of *non-LTE Hopf functions* carefully chosen to ensure the flux conservation better than 2 % at any depth point; rate equations are solved in the co-moving frame scheme, with the coupling between the radiation field and the rate equations solved using local ALOs (following Puls 1991). This new version includes the effects of the *line blanketing*. The reader is referred to Puls et al. (2003, in preparation) for a detailed description. We have analysed two Galactic stars, 10 Lac (O9V) and HD209975 (O9.5Ib) in order to compare our results with the ones obtained with other codes. In the case of 10 Lac, our results agree with the recent ones by Herrero, Puls & Najarro (2002, see their comparison to the results by Hubeny et al. 1998). The derived parameters for HD209975 are consistent with the results by Villamariz et al. (2002) which used plane-parallel model with line blocking.

A model is prescribed by the effective temperature T_{eff} , the surface gravity $\log g$, the stellar radius R_* (all these three quantities are defined at $\tau_{Ross.} = 2/3$), the mass-loss rate \dot{M} , the wind terminal velocity v_∞ , the β exponent of the wind velocity law, the He abundance Y_{He} , the microturbulent velocity v_{turb} and, in the case of B-type stars, the Si abundance. The T_{eff} is well determined from the Si III triplet and the blends of Si IV (with O II at 4090 Å and with O II/He I at 4120 Å), and the surface gravity from the Balmer hydrogen lines, provided that the mass-loss rate information is extracted from the H α profile. An important issue concerns the wind terminal velocity, that must be adopted from a spectral type - v_∞ empirical calibration (Haser 1995; Kudritzki & Puls 2000). The assumed terminal velocity affects the derived \dot{M} and the $\log g$. But, with the joined information from H α and H β , the mass-loss rate and v_∞ can be constrained to yield reasonable uncertainties in $\log g$. The stellar radius is derived interactively from the absolute magnitude, deduced from the apparent magnitude after adopting a distance modulus ($\mu = 26.53$, Freedman et al. 2001), and the model emergent flux (Kudritzki et al. 1999), which also provides the reddening by the comparison of the synthetic colors with the observed ones.

3.2. Results

Best-fitting models are displayed in Fig. 1 and the results summarized in Tab. 1. The derived β values are consistent with those obtained by Kudritzki et al. (1999) for Galactic B-Sg, with lower values excluded by the arise of emission wings in the synthetic H α profiles. We estimated an uncertainty of ± 0.25 in β . In the case of B-12 only the higher Balmer

lines have been considered in the surface gravity determination, as the cores of $H\gamma$ and $H\beta$ are particularly affected by the sky subtraction. As it has been quoted, the O and N abundances are very well constrained because of the large number of features from these species. The presence of a lot of weak metal lines in the 4600 - 4700 Å wavelength range makes the selection of the continuum level in this area difficult, good S/N ratio is also needed to disentangle between a real feature and the noise effects. Final abundance uncertainties are estimated to be ± 0.2 dex from model comparisons (see Fig. 2).

We define the mean metallicity as the sum of the α -elements abundances, $X_{Si}+X_{Mg}+X_O$ and refer it to the Sun abundances by Grevesse & Sauval (1998); at the early stages of massive star evolution, the O surface abundance is not affected by the CNO cycle, which means that the abundance of the α -elements is a direct measurement of the ZAMS metallicity of the star. The results for B-12, located close to the galactic center, resembles the abundance patterns of the early B-Sg in the solar neighborhood, having a solar metallicity within the uncertainties of the analysis. On the other hand A-9, in the outskirts of the galaxy, has clearly a lower metallicity, around $0.3 Z_{\odot}$. This is in agreement with the results for A-8, a B9-A0 supergiant close to A-9, by Bresolin et al. (2002a, see the Fig. 2). These authors find a mean metallicity of $0.2 Z_{\odot}$ for A-8. We must emphasize that both the model atmospheres and the metallicity indicators are different, but the results agree extremely well. The metallicity and the spatial location of both stars in NGC 300 points to a M33-like radial metallicity gradient. The CNO abundances indicate a different degree of chemical evolution, while B-12 displays a normal CNO spectrum, A-9 shows indications of strong N enrichment.

Synthetic magnitudes and colors (see Tab. 2) are consistent with almost no reddening for both stars, except the observed $(V - I)$ for B-12 that seems to be anomalous, probably reflecting the presence of the H II region. Fig. 3 shows the location of the stars on the Hertzsprung-Russell diagram, along with theoretical stellar tracks without rotation at solar metallicity from Schaller et al. (1992). We have also added the location of the Galactic stars 10 Lac, HD209975 and HD14956 as a reference.

Comparing the wind momentum of both NGC 300 stars with the results for Galactic supergiants (Fig. 4), B-12 agrees well with the results by Herrero et al. (2002) for O-type supergiants in the Galactic association Cyg OB2, as does HD14956. Note, however that the Herrero et al. (2002) stars are considerably hotter than the ones considered here. The wind momentum of A-9 is also compatible with the WLR of Galactic early B-Sg as derived by Kudritzki et al. (1999). With respect to this relationship, however, B-12 (being an early B-type supergiant as well) shows an enhanced wind momentum rate, which might be related to clumping effects in the wind that would produce an overestimation of the mass-loss rate. The failure of our models to reproduce the blue absorption of $H\alpha$ for B-12, in parallel with

an $H\gamma$ core which is too strongly refilled might then be explained by this effect, at least in part, and not only by the rather problematic sky subtraction outlined above. The location of A-9, compared to HD14956, reflects the lower metal content of the NGC 300 supergiant. It must be considered here that we have adopted the same v_∞ for both stars, HD14956 and A-9, while a lower value for A-9 could be expected due to its lower metallicity (Kudritzki & Puls 2000). In any case the effect of the lower wind terminal velocity would reduce even more the wind momentum of A-9, reinforcing the difference with respect to the Galactic B1.5Ia.

Recently Kudritzki, Bresolin & Przybilla (2003) have proposed a new extragalactic distance indicator, the "Flux-weighted - Luminosity Relationship (FGLR)". The results for both NGC 300 B-type supergiants, B-12 and A-9, follow this relationship, within the observed scatter (see the Fig. 2 of the latter reference).

We are grateful to L. J. Corral for making us available the spectrum of HD14956. MAU thanks F. Najarro for providing the routines for the computation of the synthetic magnitudes. AH and MAU thank the Spanish MCyT for a support under proyect PNAYA2001-0436, partially funded with FEDER funds from the EU. WG gratefully acknowledges financial support for this work from the Chilean Center for Astrophysics FONDAP 15010003.

REFERENCES

- Bresolin, F., Kudritzki, R.-P., Méndez, R. H., & Przybilla, N. 2001, *ApJ*, 548, 149
- Bresolin, F., Gieren, W., Kudritzki, R.-P., Pietrzyński, G., & Przybilla, N. 2002a, *ApJ*, 567, 277
- Bresolin, F., Kudritzki, R.-P., Najarro, F., Gieren, W. & Pietrzyński, G. 2002b, *ApJ*, 577, L107
- Freedman, W. L., et al. 2001, *ApJ*, 553, 47
- Grevesse, N. & Sauval, A. J. 1998, *Space Sci. Rev.*, 85, 161
- Haser, S. M. 1995, Ph.D. thesis, Ludwig-Maximilians Univ., Munich
- Herrero, A., Puls, J., & Najarro, F. 2002, *A&A*, in press
- Hubeny, I., Heap, S. R., & Lanz, T. 1998, *ASP Conf. Series Vol 131*, 108
- Kewley, L. J. & Dopita, M. A. 2002, *ApJS*, 142, 35

- Kudritzki, R.-P., et al. 1999, A&A, 350, 970
- Kudritzki, R.-P. & Puls, J. 2000, ARA&A, 38, 613
- Kudritzki, R.-P., Bresolin, F., & Przybilla, N. 2003, ApJ, 582, 83
- Monteverde, M. I., Herrero, A., & Lennon, D. J. 2000, A&A, 545, 813
- Pilyugin, L. S. 2002, preprint (astro-ph/0211319)
- Przybilla, N. 2002, Ph.D. thesis, Ludwig-Maximilians Univ., Munich
- Puls, J. 1991, A&A, 248, 581
- Santolaya-Rey, E., Puls, J., & Herrero, A. 1997, A&A, 323, 488
- Schaller, G., Schaerer, D., Meynet, G., & Maeder, G. 1992, A&AS, 96, 269
- Smartt, S. J., Dufton, P. L., & Lennon, D. J. 1997, A&A, 326, 763
- Smartt, S. J., Lennon, D. J., Kudritzki, R.-P., Rosales, F., Ryans, R. S. I., & Wright, N. 2002, A&A, 979, 991
- Takeda, Y. & Takada-Hidai, M. 1998, PASJ, 50, 629
- Venn, K. A. 1995, ApJ, 449, 839
- Villamariz, M. R., Herrero, A., Becker, S. R., & Butler, K. 2002, A&A, 388, 940
- Vink, J. S., de Koter, A., & Lamers, H. J. G. L. M. 2000, A&A, 362, 295

Table 1. Best-fit model parameters

ID	Teff <i>kK</i>	log g <i>dex</i>	R R_{\odot}	Y_{He}	v_{turb} <i>km s⁻¹</i>	v_{∞} <i>km s⁻¹</i>	\dot{M} $10^{-6} M_{\odot} yr^{-1}$	β	ϵ_{Si} <i>dex</i>	ϵ_O <i>dex</i>	ϵ_{Mg} <i>dex</i>	ϵ_N <i>dex</i>	ϵ_C <i>dex</i>	Z Z_{\odot}	[<i>M/H</i>] dex	$log(L/L_{\odot})$ <i>cgs</i>
B-12	24.0±1.0	2.60±0.15	43.5±1.5	0.10	20.	1500.	3.00±0.50	1.50	7.45	8.65	7.50	7.50	8.00	1.00	0.00	5.75±0.10
A-9	21.0±1.0	2.50±0.15	32.0±1.0	0.10	15.	800.	0.25±0.07	2.00	7.10	8.30	7.20	8.00	7.60	0.30	-0.50	5.24±0.11

Note. — The metal abundances are expressed as $\epsilon_A = 12 + \log(A/H)$, while $[M/H] = (M/H)_{*} - (M/H)_{\odot}$.

Table 2. Observed and synthetic magnitudes and colors.

ID	Observed			Synthetic				$E(B - V)$	$E(V - I)$
	V	$B - V$	$V - I$	M_V	$M_B - M_V$	$M_V - M_I$	BC		
B-12	19.30	-0.18	0.00	-7.29	-0.17	-0.23	-2.33	0.00	0.23
A-9	20.23	-0.17	...	-6.36	-0.16	-0.20	-1.97	0.00	...

Note. — We have adopted a distance modulus $\mu = 26.53 \pm 0.07$ (Freedman et al. 2001).

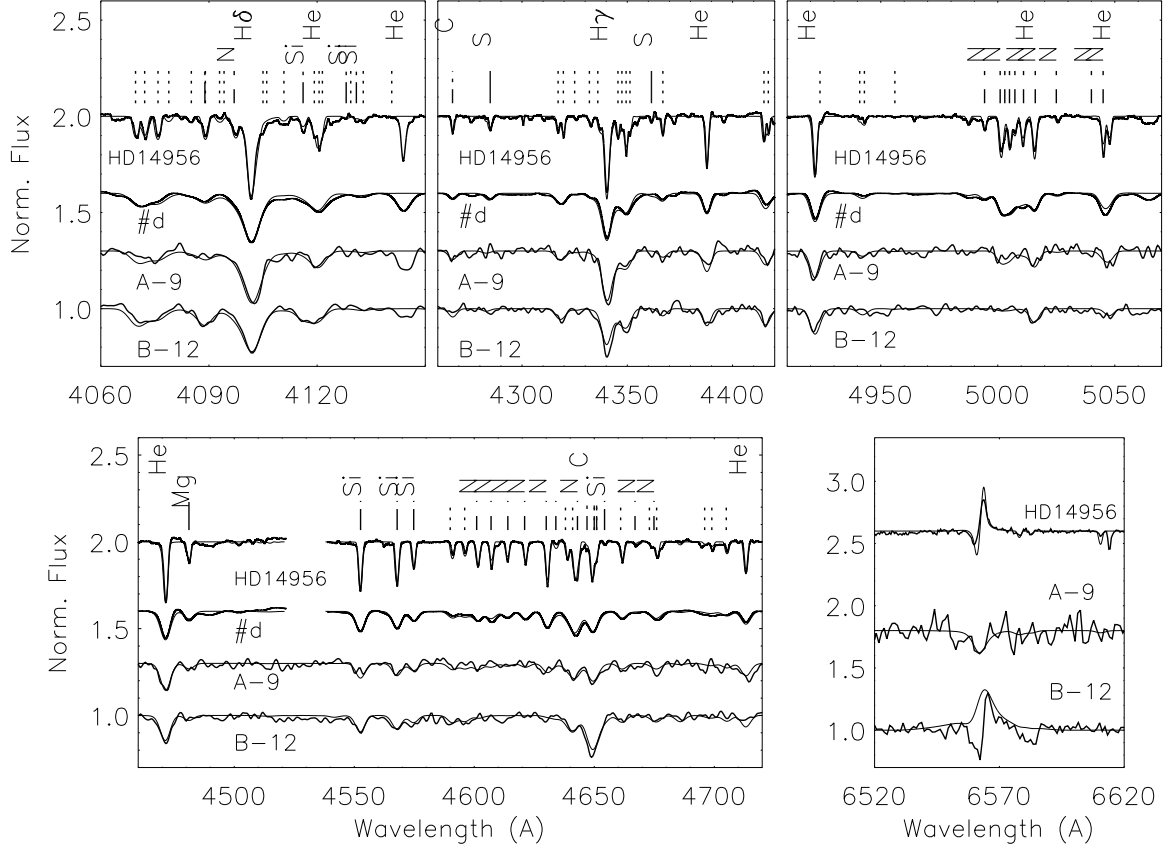


Fig. 1.— Observed spectra of B-12 and A-9, the Galactic B-type supergiant HD14956, the same spectrum degraded to the NGC 300 data resolution and the final fits. The spectra have been shifted for the sake of clarity. An identification of most prominent features are given: O (dotted, without labels), Si (dashed-dotted-dotted), N (dashed), C (dashed-dotted-dashed), Mg (solid), H and He.

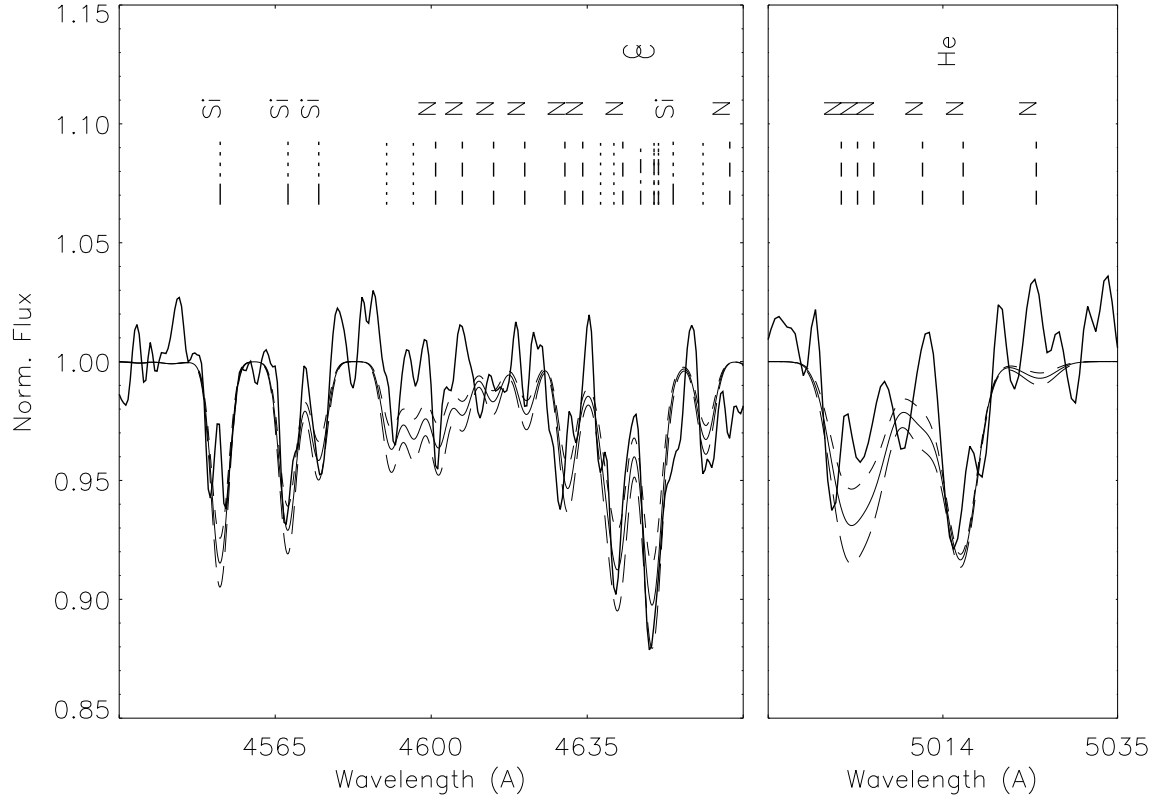


Fig. 2.— Selected regions of the observed spectrum of A-9, the final fit and two models at ± 0.2 dex to illustrate the uncertainties of the analysis. Line identification as in the previous figure.

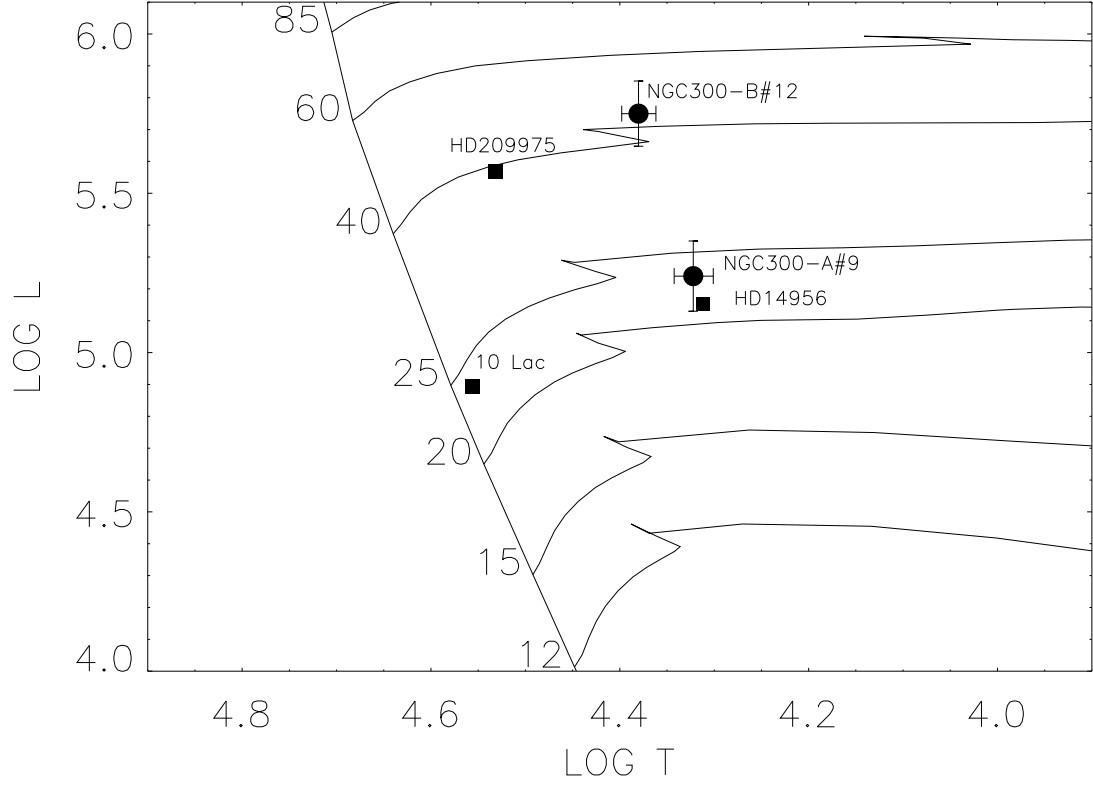


Fig. 3.— Location of the NGC 300 B-type supergiants in the HR diagram. We have also added the Galactic stars HD14956, HD209975 and 10 Lac. The theoretical stellar tracks without rotation at solar metallicity are taken from Schaller et al. (1992). Note that A-9 has a metallicity of only $0.3Z_{\odot}$.

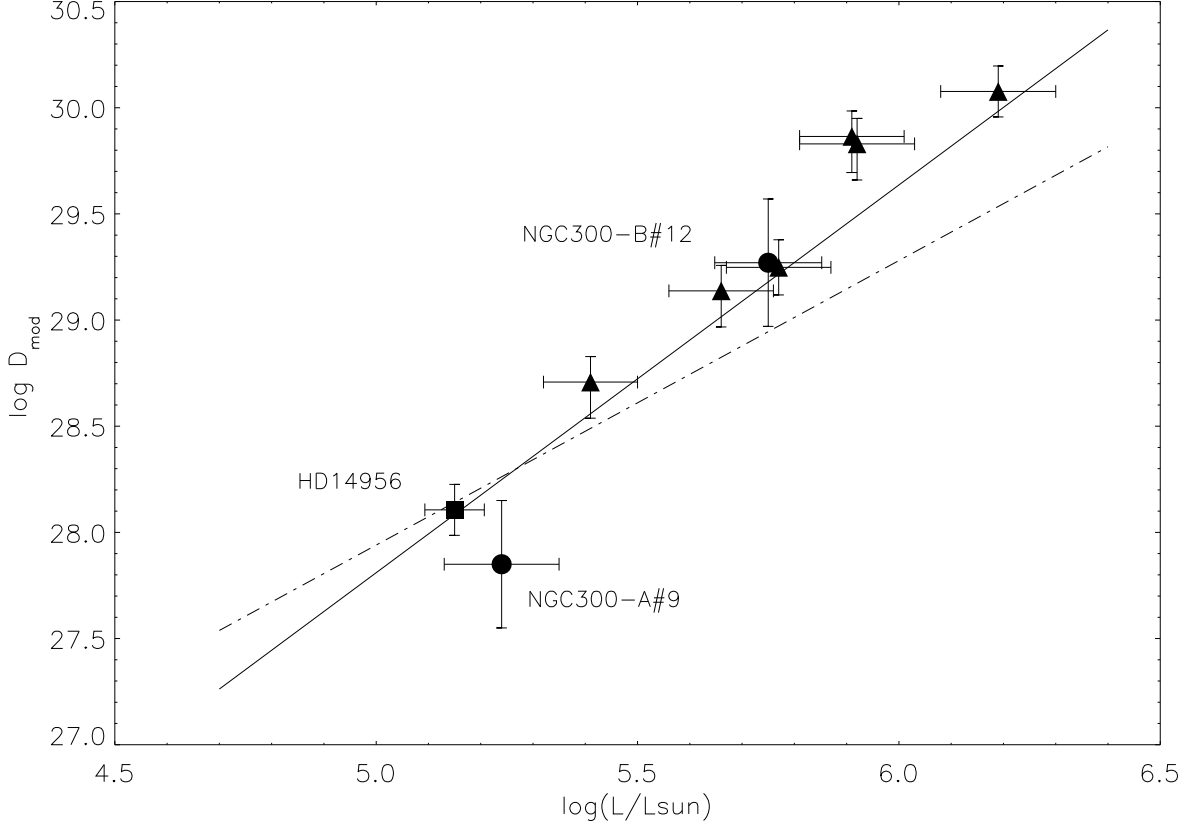


Fig. 4.— Wind momentum - Luminosity Relationship. Filled circles stand for the NGC 300 stars and the square denotes HD14956, while the triangles represent the Cyg OB2 OB supergiants from Herrero et al. (2002). Solid line is the theoretical prediction by Vink, de Koter, & Lamers (2000) for $T_{\text{eff}} \geq 27500$ K, and the dashed-dotted line is the fit to the Galactic early B-type supergiant data from Kudritzki et al. (1999). The modified wind momentum is defined as $D_{\text{mod}} = \dot{M}v_{\infty}(R_{*}/R_{\odot})^{1/2}$.